Technibaryon production at pp colliders

Antonio Dobado
Departamento de Física Teórica and Instituto de Física Fundamental, Universidad Complutense de Madrid, 28040 Madrid, Spain

Juan Terron*
Deutsches Elektronen-Synchrotron DESY, Notkestrasse 85, 2000 Hamburg 52, Germany
(Received 5 June 1991; revised manuscript received 8 July 1991)

If the symmetry-breaking sector of the standard model is strongly interacting, the low-energy dynamics of the longitudinal components of the weak bosons can be described by a nonlinear σ model with two free parameters. For a large range of these parameters the model supports finite-energy solitons called weak Skyrmions or technibaryons. Technibaryons could be produced at the Superconducting Super Collider giving rise to exotic experimental signatures since they are stable, heavy, and in some cases, fractional-charged particles.

PACS number(s): 13.85.Qk, 12.50.Lr, 14.80.Pb

I. INTRODUCTION

One of the main goals of the next generation of pp colliders [the CERN Large Hadron Collider (LHC) and the Superconducting Super Collider (SSC)] is to bring some light on the nature of the symmetry-breaking sector (SBS) dynamics of the standard model (SM). This is especially true if this dynamics is strongly interacting [1]. In this case the only light particles of the SBS will be the longitudinal components of the gauge bosons (W_L), the rest of the particles or resonance being in the TeV region. The mass gap between the W_L's and the TeV scale may be understood in that case by assuming the existence of some global symmetry G of the SBS. This symmetry is spontaneously broken into some group H with $H \subset G$, the W_L's being the Goldstone bosons associated with this global symmetry breaking [2].

Because of the gauge symmetry-breaking pattern of the SM, $SU(2)_L \times U(1)_Y \to U(1)_{em}$, it is clear that $SU(2)_L \times U(1)_Y$ has to be a subgroup of G and $U(1)_{em}$ has to be a subgroup of H. On the other hand, since the ρ parameter is close to one, H has to contain the so-called custodial symmetry SU(2) [3], which in a natural way gives $\rho \sim 1$ in the SBS. With the above constraints, the more natural and simplest choice for G and H is $G = SU(2)_L \times SU(2)_R$ and $H = SU(2)_{L+R}$.

In this case the low-energy dynamics of the SBS can be described by a phenomenological Lagrangian [4] or the so-called chiral perturbation theory (ChPT) which has proved to be very useful in the hadron physics context [5]. In this approach the Goldstone-boson interactions are described by a Lagrangian which is an expansion in the number of the derivatives of the fields. The first term of this expansion (two derivatives) is universal; i.e., it is not dependent on the SBS dynamics provided it is strong. On the contrary free parameters appear in successive terms encoding the information about the SBS dynamics. ChPT has been applied recently to the study of the $W_L W_L$ scattering at the LHC and SSC [6], and it has been shown how it could be possible to determine some of the parameters of the chiral expansion and get information about the SBS dynamics in these colliders.

In this work, we will follow a similar philosophy but we will concentrate on the so-called nontrivial sector of the model. As we will see, certain SBS dynamics are such that the corresponding chiral Lagrangians support topologically stable solitons [7] which could provide a description of part of the spectrum of the SBS dynamics. These solitons (called Skyrmions in the literature) are well known in the hadron physics context where they correspond to baryons. Most of the properties of these particles are well described by the Skyrmion model [8] at least in a qualitative level. In the case of the SBS dynamics of the SM we do not know if such solitons (weak Skyrmions or technibaryons [9]) exist or not because this depends on the values of the parameters appearing in the chiral Lagrangian and these are by now completely undetermined. Nevertheless, it is a matter of fact that the existence of these weak Skyrmions is a generic prediction of the chiral Lagrangians, as applied to the SBS dynamics of the SM, for a very large region of the parameter space.

This being so, we will focus our interest in this work on the possibility of producing and detecting such particles at the LHC and SSC. By the use of some reasonable physical hypothesis we will compute the production cross section of weak Skyrmions in these machines in terms of the chiral Lagrangian parameters only. We will see that weak-Skyrmion production at the SSC can be important in many models, such as, for instance, those based on a theory analogous to QCD such as technicolor.

II. TECHNIBARYON PROPERTIES

Following the ideas of the discussion above we start by considering the more general low-energy action for the

*On leave of absence from Department de Física Teórica de la Universidad Autónoma de Madrid, 28049 Madrid, Spain.

Goldstone bosons associated with the global-symmetry-breaking pattern $SU(2)_L \times SU(2)_R \to SU(2)_{L+R}$:

$$S=\int d^4x\,\mathcal{L}(x)+n\pi\delta[U]\,, \tag{1}$$

where

$$\mathcal{L}(x)=-\frac{v^2}{4}\,\mathrm{tr}V_\mu V^\mu+M\,\mathrm{tr}(V_\mu V^\mu)\,\mathrm{tr}(V_\nu V^\nu) +N\,\mathrm{tr}(V_\mu V^\nu)\,\mathrm{tr}(V^\mu V_\nu)\,. \tag{2}$$

Here $V_\mu \equiv \partial_\mu U\,U^\dagger, U(x)=\exp[i\sigma^a w^a(x)/v]$ with $w^a(x)$ being the Goldstone-boson field and σ^a the Pauli matrices. The functional $\delta[U]$ is equal to zero if U belongs to the trivial class of $\pi_4(SU(2))$ and equal to one if it belongs to the nontrivial one [recall that $\pi_4(SU(2))=Z_2$]. This contribution to the action is reminiscent of the Wess-Zumino [10] term and it was introduced in this context in [11]. The information about the underlying theory is encoded in the M and N parameters and in the integer n. As is well known from hadron physics, one of the most important features of the model considered here is the possibility of the existence of static, topologically stable, finite-energy solutions (the above-mentioned weak Skyrmions or technibaryons). This is so because any static finite-energy $U(\mathbf{x})$ field must belong to some homotopy class labeled by an integer number [recall that $\pi_3(SU(2))=z$] given by

$$t[U]=\frac{1}{24\pi^2}\int d^3x\,\epsilon^{ijk}\,\mathrm{tr}(V_iV_jV_k)\,. \tag{3}$$

This number is additive and conserved in the limit we are considering here (we are neglecting any gauge coupling) and we will call it the technibaryon number in close analogy with the case of the Skyrmion in hadron physics. In order to obtain a nonzero size and positive-energy solutions, further conditions have to be introduced on the parameters M and N. Using the standard notation in Skyrmion physics, these conditions read $e^2\equiv 1/(16N)>0$ and $\gamma\equiv(1+M/N)/2<0$ [12]. Therefore, the existence of technibaryons does not seem to be a rare feature of the models considered here since they appear in a very large region of parameter space. For any given values of the parameters in that region, the classical mass of the technibaryon can be obtained by minimizing the mass functional

$$M[U]=-\int d^3x\,\mathcal{L}(\mathbf{x})\,. \tag{4}$$

For the $t=1$ sector, it is useful to use the standard ansatz for the Skyrmion field $U_S(\mathbf{x})=\exp[if(r)\hat{x}_a\sigma_a]$ being $f(0)=\pi$ and $f(\infty)=0$ the right boundary conditions for the chiral angle $f(r)$. The low-energy spectrum of the weak Skyrmion can be computed in the usual way studying the collective excitations of the zero modes (rotations and isorotations) [8]. The following Hamiltonian is obtained:

$$H=M_{\mathrm{cl}}+\frac{\hat{J}^2}{2\Lambda}=M_{\mathrm{cl}}+\frac{\hat{I}^2}{2\Lambda}\,, \tag{5}$$

where $\hat{J}^2=\hat{I}^2$ are the squared spin and isospin operators and M_{cl} and Λ are the classical mass and the moment of inertia of the weak Skyrmion, which can be computed numerically. For $|\gamma|\ll 1$ it is found $M_{\mathrm{cl}}=76(1-0.77\gamma+\ldots)v/e$ and $\Lambda=53.3(1-1.1\gamma+\ldots)/(ve^3)$. Therefore, for $t=1$, the weak-Skyrmion states are determined by the quantum numbers $J=1$. Their energies are given by

$$H|J\rangle=\left[M_{\mathrm{cl}}+\frac{J(J+1)}{2\Lambda}\right]|J\rangle\,. \tag{6}$$

In order to determine the possible values of J we have to know if technibaryons are bosons or fermions. In principle these two possibilities are open. This is so because the configuration space Q in this problem is $Q=\{U:S^3\to SU(2)\}$. The way in which technibaryons have to be quantized lies in the nature of the first homotopy group of Q, i.e., $\pi_1(Q)$. The possibility of defining multivalued wave functions on Q, which is needed for fermionic quantization, is related to having a nontrivial $\pi_1(Q)$. This becomes clear if, for instance, a 2π rotation (which is a loop in Q) is considered. In our case $\pi_1(Q)=Z_2$ and this means that technibaryons may be quantized as bosons or as fermions. In the first case $I=J$ take the values $0,1,2,\ldots$ and in the second $I=J=\frac{1}{2},\frac{3}{2},\ldots$. In fact, having bosonic or fermionic quantization depends on the value of n in Eq. (1). This is so because, as is shown in [10], a process containing a 2π rotation of a Skyrmion has $\delta[U]=1$ and therefore the amplitude for such a rotation picks up a factor $(-1)^n$ from the second term in Eq. (1) that can be understood as a $\exp(i2\pi J)$ factor. In summary, if n is even, technibaryons are bosons but if n is odd technibaryons are fermions. Of course, in the last case, other fermions should be introduced in the model in order to cancel the local and global anomalies that otherwise would be present. In the following we will not consider these new fermions because their nature and properties are model dependent and we will keep our analysis as general as possible.

In the above discussion, we have not taken into account the effect of loops of the Goldstone bosons on the features of the technibaryons. The effects of these loops in the W_LW_L scattering have been considered by the authors, along with Herrero [6], by the use of well-known techniques of ChPT. More recently, one-loop effects in the mass of the Skyrmion have been taken into account by the use of a nonlocal effective Lagrangian $\mathcal{L}_{\mathrm{eff}}$ [12]. When one-loop effects are incorporated, one has to change $\mathcal{L}(x)$ by $\mathcal{L}_{\mathrm{eff}}(x)$ in Eq. (4). Then the mass functional becomes a very complex nonlocal functional because of the nonlocality of $\mathcal{L}_{\mathrm{eff}}$ (see [12] for the display of the complete formula). It is very useful in this case to use some parametrization of the chiral angle such as the one by Atiyah and Manton [13]:

$$f_R(r)=\pi[1-(1+R_S^2/r^2)^{1/2}]\,, \tag{7}$$

where the parameter R_S is a measure of the size of the Skyrmion. Another important outcome of including one-loop effects is that the bare constants M and N become renormalized constants $M(\nu)$ and $N(\nu)$ which are well-defined functions of some arbitrary renormalization scale ν. Of course, physical magnitudes such as scatter-

ing amplitudes or Skyrmion masses do not depend on this scale.

Giving different values to the renormalized constants $M(v)$, $N(v)$, and to the integer n, one can reproduce the low-energy behavior of different underlying SBS dynamics. Three typical models for the SBS dynamics often considered in the literature are the following.

(a) The minimal standard model (MSM), where the symmetry breaking is driven by a Higgs doublet. In this case, the Goldstone-boson scattering amplitudes to one loop [14] are reproduced by the chiral model taking

$$M(m_H)=\frac{1}{8(4\pi)^2}\left[\frac{9\pi}{2\sqrt{3}}-\frac{74}{9}\right],$$
$$N(m_H)=\frac{-1}{18(4\pi)^2}, \tag{8}$$

where $m_H^2=2\lambda(m_H)v^2$, $\lambda(v)$ being the one-loop running coupling constant corresponding to the self-interactions of the Higgs boson (here we have assumed $m_H \gg v$). Furthermore, n has to be taken equal to zero.

(b) The QCD-like models, where the SBS dynamics is a rescaled version of QCD ($f_\pi \to v$). This is the simple physical idea underlying technicolor theories [15]. The chiral Lagrangian parameters are obtained from the QCD ones (see below):

$$M^{\mathrm{QCD}}(1\ \mathrm{GeV})=-0.0027,$$
$$N^{\mathrm{QCD}}(1\ \mathrm{GeV})=-0.0011, \tag{9}$$
$$n=3.$$

These values are chosen to fit the $\pi\pi$ scattering data [16] (see also [17] for an alternative fit) and $n=3$ from the 3 colors of QCD [10].

(c) Technicolor models: By the use of large-N arguments one can extend the QCD-like case to the case with an arbitrary number of colors (technicolors) N_{TC}. Then

$$M^{\mathrm{TC}}\left[\frac{v}{f_\pi}\left[\frac{3}{N_{\mathrm{TC}}}\right]^{1/2}v\right]=\frac{N_{\mathrm{TC}}}{3}M^{\mathrm{QCD}}(v),$$
$$N^{\mathrm{TC}}\left[\frac{v}{f_\pi}\left[\frac{3}{N_{\mathrm{TC}}}\right]^{1/2}v\right]=\frac{N_{\mathrm{TC}}}{3}N^{\mathrm{QCD}}(v), \tag{10}$$
$$n=N_{\mathrm{TC}}.$$

Please note the difference between $N^{\mathrm{TC}}(v)$ which is a renormalized coupling constant and N_{TC} which is the number of technicolors.

Once we have the values of the chiral parameters corresponding to the models above, one can find numerically the value of R in Eq. (7) that leads to the minimum of the mass functional and obtain the technibaryon mass for them. Nevertheless, we have to be careful since the stability of the technibaryon is not guaranteed in all cases. For instance, in [12] it is argued that, in the QCD-like case, technibaryons are very likely to be stable, but numerical analysis done by the authors show that this is not the case in the MSM. Therefore, technibaryons or weak Skyrmions are more likely to be relevant in technicolor theories than in the MSM where they probably do not exist at all. For the sake of definiteness we will concentrate on those theories in the following but our main results are, by far, much more general.

Until now we have neglected the coupling of the Goldstone bosons to the gauge fields corresponding to the local $\mathrm{SU}(2)_L \times \mathrm{U}(1)_Y$ symmetry of the SM. Some of the effects produced by these fields on the weak Skyrmions have been considered in [18] at classical level. Mainly they concern with the stability region in the parameter space. For instance, in the case $\gamma=0$, weak Skyrmions become unstable if $e^2>1.17$ (note that this will never be the case in the technicolor models that will be considered here). Another effect of the gauge fields is that the topological current becomes anomalous and the technibaryon number is not conserved anymore, being violated by instantonic transitions. Nevertheless, these transitions are expected to be very suppressed as happens in the baryonic Skyrmion [19] and, therefore, they will not be taken into account here.

Let us consider now the problem of the determination of the electric charge Q of the technibaryons. By switching on the electromagnetic field it has been shown perturbatively that Q has to be equal to the third component of the isospin I_3 (see Eilam and Stern in [18]). As long as I_3 is an integer or half-integer, this result must be true nonperturbatively too.

Finally, we are able to collect the main quantum numbers of the technibaryons. For every t sector we have, in principle, a tower of states characterized in the bosonic case by $I=J=0,1,2,\ldots$ and in the fermionic case by $I=J=\frac{1}{2},\frac{3}{2},\ldots$, the electric charge of any (iso)multiplet being given by $Q=I_3$. The quantum numbers of the antitechnibaryons are obtained as usual from those corresponding to the technibaryons (this of course includes a change in the sign of t). The possibility of having other nonzero quantum numbers such as the baryonic number or ordinary color is much more model dependent. In fact these other quantum numbers will give rise to many other channels for producing technibaryons that will not be considered in this work. The reason is that we want to make an analysis as general as possible. According to our philosophy the only common ingredient in any realistic model is the chiral symmetry mentioned in the Introduction. Thus the only technibaryon interactions that will be taken into account are pure chiral interactions and not the ones corresponding to other quantum numbers.

III. TECHNIBARYON PRODUCTION CROSS SECTIONS

Let us concentrate now on the problem of how these technibaryons could be produced at high energies in pp collisions (see Fig. 1). The first important fact to take into account is that the technibaryon number has to be conserved and therefore technibaryons have to be produced in pairs (one technibaryon T and one antitechnibaryon $\bar{T}$). The next step is to obtain some effective coupling between the technibaryons and the W_L's. In the following, we will assume that the technibaryons, which are extended objects of size R_S, can be considered as pointlike particles and can be described by local fields.

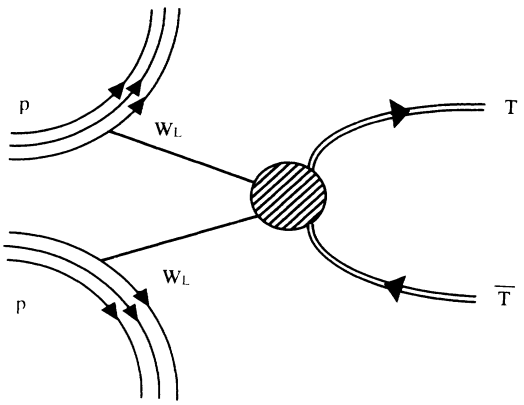

FIG. 1. Pictorial view of the production of technibaryons in pp collisions.

This approach is appropriate if the dynamical cross section for the elastic scattering $W_L T$ is much more large than the geometrical one, i.e., πR_S^2. As we have checked numerically, this is the case for the physical situations relevant for us in this paper.

The kind of field needed to describe technibaryons in the local approximation depends of course on the spin of these objects. In the bosonic case the stable technibaryon has $I=J=0$ and $|t|=1$ so it has to be described by a complex scalar field ϕ. Note that technibaryons with higher values of (iso)spin would decay, in principle, in the stable one ($I=J=0$) by emitting photons, $W^{\pm}$ and Z^0 bosons since t is conserved in these processes. The coupling of the scalar technibaryon ϕ to the W_L field can be described by the Lagrangian

$$\mathcal{L}_{\text{int}}=\alpha\phi\phi^* \operatorname{tr}(\partial_\mu U\, \partial^\mu U^\dagger) . \tag{11}$$

This Lagrangian is chiral invariant and has only two derivatives of the W_L field so it is the relevant one at low energies. The constant α is obtained from the long-distance behavior of the Skyrmion solution which is given by

$$U(x)=1+\frac{i}{r^2}B\hat{x}^a\sigma^a+\cdots . \tag{12}$$

For instance, $B=R_S^2\pi/2$ in the parametrization of Atiyah and Manton. R_S is the value that minimizes the mass functional and it is a measure of the size of the Skyrmion. The value of α needed in Eq. (11) to produce the same w_a field at large distances with a punctual source is given by $\alpha=-\frac{4}{3}\pi^2 v^4 B^2$ [20]. Thus we can obtain α as function of $M(v)$ and $N(v)$ and hence we can compute the $w_a T$ coupling corresponding to different underlying SBS dynamics. From the Lagrangian in Eq. (11) we find the Feynman rule [see Fig. 2(a)]

$$w_a(p_1)w_b(p_2)\to\phi\phi^* \sim i\frac{4\alpha}{v^2}p_1\cdot p_2\delta_{ab} \tag{13}$$

so the cross section for the process $w_a w_a\to\phi\phi^*$ is given by

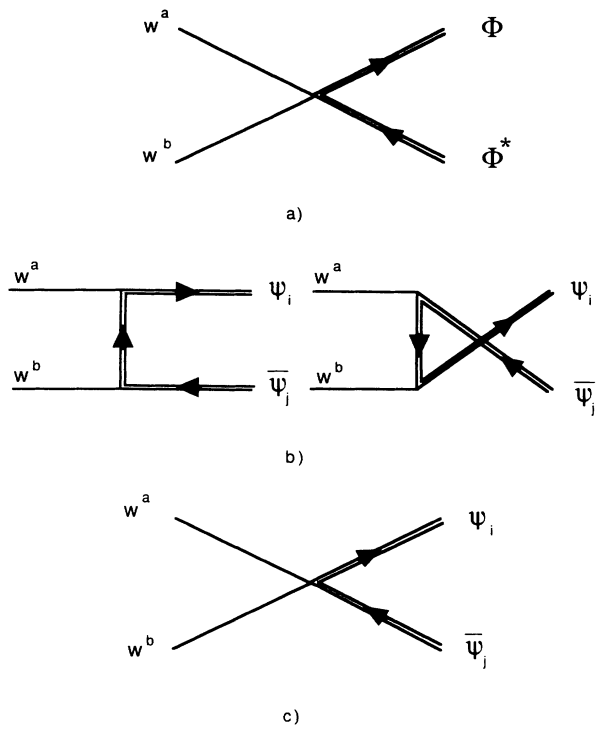

FIG. 2. Feynman diagrams contributing to the production of technibaryons from the longitudinal components of the gauge bosons: (a) bosonic case; (b) fermionic case (axial-vector coupling); (c) fermionic case (vectorial coupling).

$$\frac{d\sigma}{d(\cos\theta)}=\frac{\alpha^2 s}{8\pi v^4}\left[\frac{s-4m_\phi^2}{s}\right]^{1/2}=\frac{\pi^7}{72}v^4 R_S^8 s\left[\frac{s-4m_\phi^2}{s}\right]^{1/2} \tag{14}$$

with m_ϕ being the scalar-technibaryon mass. This cross section corresponds to an S-wave channel with total isospin equal zero. It is the leading order of an expansion in terms of the technibaryon velocity $\beta=\sqrt{1-4m_\phi^2/s}$.

In the fermionic case the stable technibaryon has $I=J=\frac{1}{2}$ so it is described by a doublet of spinors ψ_i where $i=I_Z$ take the values $\frac{1}{2}$ or $-\frac{1}{2}$. The low-energy chiral-invariant coupling to the W_L field can be obtained as follows. We define the object $\mathcal{V}^\mu=\partial^\mu\mathcal{U}\,\mathcal{U}^\dagger$ where $\mathcal{U}=\exp[i\gamma^5\sigma^a w^a(x)/v]$. Then, the more general $\mathrm{SU}(2)_{L+R}$-invariant interacting Lagrangian with one derivative acting on the w^a fields is given by

$$\mathcal{L}_{\text{int}}=-ik\bar{\psi}\not{\mathcal{V}}\psi , \tag{15}$$

where ψ is the isodoublet and k is an arbitrary coupling constant. Expanding the exponential appearing in the definition of $\mathcal{U}$ we get

$$\mathcal{L}_{\text{int}}=\frac{k}{2v}\mathbf{A}_\mu\cdot\partial^\mu\mathbf{w}-\frac{k}{4v^2}\mathbf{V}_\mu\cdot(\mathbf{w}\times\partial^\mu\mathbf{w})+\cdots , \tag{16}$$

where $\mathbf{A}_\mu=\psi\gamma_\mu\gamma^5\boldsymbol{\sigma}\psi$ and $\mathbf{V}_\mu=\bar{\psi}\gamma_\mu\boldsymbol{\sigma}\psi$ are the axial-vector and vector currents associated with the fermionic isodoublet. The rest of the terms have more than two w^a

fields and will be neglected. Therefore, we have in principle two interacting terms depending on one coupling constant k. By the use of the equations of motion, it is not difficult to realize the following: given a distribution of the ψ field (the Skyrmion in our case) located around some point in the space, the produced w^a field at large distances from this point is dominated by the axial-vector coupling in Eq. (16). By comparison with the value of the w^a field at large distances corresponding to the Skyrmion solution it is not difficult to find $k=\frac{8}{3}\pi v^2 B$ [8].

Note that in this case one would need to use Eq. (5) to compute m_ψ and this requires the calculation of the moment of inertia Λ of the weak Skyrmion. Although this is not difficult in the classical case, it turns out to be a very hard task when one-loop corrections are included. In any case, the contribution coming from the $J(J+1)/(2\Lambda)$ term in Eq. (5) is not expected to be very large. From our experience in QCD we know that it is smaller than the uncertainties of the whole approach followed here. Therefore, we will neglect its contribution to the mass of the fermionic technibaryon m_ψ (see next paragraph for the values of the technibaryon masses used in our numerical computations). The Feynman rule obtained from Eq. (15) corresponding to the axial-vector coupling is

$$w^1 \to \bar{\psi}_j \psi_i \sim \frac{k m_\psi}{v} \gamma^5 (\tau^a)_{ij} \ . \tag{17}$$

The contribution to the amplitude for the process $w^a w^b \to \bar{\psi}_j \psi_i$ is given by the Feynman diagram shown in Fig. 2(b). In addition we have in principle also the contribution coming from the vectorial coupling [Fig. 2(c)]. By the use of standard techniques it is easy to write down the amplitude for the processes $w^a w^b \to \psi_i \bar{\psi}_j$ which is given by

$$i\mathcal{M}=\bar{u}_1 \left[-i \left(\frac{k m_\psi}{v} \right)^2 \left(\frac{\not q - m_\psi}{t-m_\psi^2} A + B \frac{\not q' - m_\psi}{u-m_\psi^2} \right) + \frac{k}{4v^2} \epsilon_{abc} (\tau^a)_{ij} (\not p_a - \not p b) \right] v_2 \ , \tag{18}$$

where $q=p_a-q_1$, $q'=p_a-q_2$, and $u_1=u(q_1,\sigma_1)$, $\bar{v}_2=\bar{v}(q_2,\sigma_2)$ are the spinors corresponding to ψ and $\bar{\psi}$. The constants A and B are

$$\begin{aligned} A &= (\tau^a)_{i,k} (\tau^b)_{k,j} \ , \\ B &= (\tau^b)_{i,k} (\tau^a)_{k,j} \ . \end{aligned} \tag{19}$$

In Eq. (18) we have used the usual expression for the propagator of a fermionic field. Nevertheless, as was explained above, we are working with a low-energy approximation. Therefore, it is inconsistent to use a propagator which contains arbitrary high powers of the technibaryon momentum. Instead, we will expand the propagators,

$$\frac{1}{m_\psi^2 - t} = \frac{1}{4m_\psi^2} \left[1 - \frac{u}{m_\psi^2} + \cdots \right] , \tag{20}$$

and we will retain only the leading terms at low energies in Eq. (18). By use of a REDUCE code we find

$$\sum_{\text{(spin)}} |\mathcal{M}|^2 = 16 \left(\frac{k m_\psi}{v} \right)^4 \left(\frac{s-4m_\psi^2}{s} \right) \cos^2\theta \ , \tag{21}$$

where θ is the angle between the proton and the technibaryon momenta in the $\psi\bar{\psi}$ c.m. system, (c.m.s.). In the computation of the isospin factors appearing in this equation we have to take into account that we are producing technibaryon-antitechnibaryon pairs. This means in particular that the total electric charge is zero and therefore the only allowed initial states are W^+W^- and ZZ. Both of them correspond to the case $a=b$ in the Cartesian basis that we are using and therefore we have in this case $\epsilon_{abc}=0$. Thus we arrive at the conclusion that the vector coupling does not contribute to the cross section of the process. The result in Eq. (21) can be compared with the one corresponding to the scalar case in the same limit which is $9(k m_\phi / v)^4/4$. Note that, in the fermionic case, the leading order in the technibaryon velocity β is a P wave channel with total momentum and isospin equal to zero. This is because the involved interaction is parity conserving. Since a fermion-antifermion system has a negative intrinsic parity, a P-wave final state is needed to keep the total angular momentum equal to zero with positive parity. This fact explains the $\beta^2 \cos^2\theta$ appearing in Eq. (21). Therefore, the formula giving the cross section for producing one fermionic technibaryon-antitechnibaryon pair is

$$\begin{aligned} \frac{d\sigma}{d(\cos\theta)} &= \frac{k^4 m_\psi^4}{2\pi s v^4} \left(\frac{s-4m_\psi^2}{s} \right)^{3/2} \cos^2\theta \\ &= \frac{128\pi^7}{81 s} v^4 R_s^8 m_\psi^4 \left(\frac{s-4m_\psi^2}{s} \right)^{3/2} \cos^2\theta \ . \end{aligned} \tag{22}$$

Once we have computed the cross section of the process $W_L W_L \to T\bar{T}$ ($T=\psi$ or ϕ) we can compute the relevant cross section for pp colliders such as LHC and SSC, i.e., $pp \to T\bar{T}+X$. To do that, we use the effective-W approximation [21]. In this approach the W_L's of the subprocess are taken to be real and the cross section of the full process is given by

$$\sigma(pp \to T\bar{T}+X) = \sum_{qq'} \int\int dx_1\, dx_2\, f_q(x_1,Q^2) f_{q'}(x_2,Q^2) \sum_a \int\int d\hat{x}_1\, d\hat{x}_2\, f_a^q(\hat{x}_1) f_b^{q'}(\hat{x}_2) \int d(\cos\theta) \frac{d\sigma}{d(\cos\theta)} \ . \tag{23}$$

Here $Q^2=x_1 x_2 S$ is the center-of-mass energy (c.m.e.) of the subprocess $qq' \to T\bar{T}$ and S is the c.m.e. of the pp system. $\hat{Q}^2=\hat{x}_1\hat{x}_2 Q^2$ if the c.m.e. of the sub-subprocess $w^1 w^b \to T\bar{T}$. f_q and $f_{q'}$ are the distribution functions of the quarks q and q' inside the proton and $f_a^q(\hat{x}_1,\hat{Q}^2)$ gives the probability for a quark q of emitting a longitudinal gauge boson a with a fraction x_1 of its energy. In the following we will use the distribution functions of [21].

Using the standard base $w^{\pm}=(w^1\mp iw^2)/\sqrt{2}$ and $z=w^3$ these functions are given by [22]

$$f_V^q(x)=c_V^q\frac{1-x}{x}\ , \tag{24}$$

where $V=W^{\pm},Z$ and

$$c_{W^{\pm}}^u=c_{W^{\pm}}^d=\frac{\alpha}{4\pi s_W^2}\ ,$$

$$c_Z^u=\frac{\alpha}{16\pi s_W^2 c_W^2}[1+(1-\tfrac{8}{3}s_W^2)^2]\ , \tag{25}$$

$$c_Z^d=\frac{\alpha}{16\pi s_W^2 c_W^2}[1+(1-\tfrac{4}{3}s_W^2)^2]\ ,$$

with $s_W^2=\sin^2\theta_W$, $c_W^2=\cos^2\theta_W$, and α being the electromagnetic coupling constant.

IV. PRELIMINARY NUMERICAL RESULTS

With the formulas given in the last paragraph we are in conditions of making a numerical estimation of the rate of production of pairs of technibaryons, both in LHC and SSC. For these machines the following values of the parameters have been taken: LHC, $\sqrt{S}=16$ TeV, $\mathcal{L}=4\times10^{34}$ cm^{-2} sec^{-1} and SSC, $\sqrt{S}=40$ TeV, $\mathcal{L}=10^{33}$ cm^{-2} sec^{-1}. In Table I the number of expected events per year for different models is shown together with the values of the mass and the radius of the produced technibaryons. Concerning the masses, the value considered here for the QCD-like model has been the rescaled mass of the proton (m_p) instead of the value obtained from the corresponding mass functional, i.e., $m_\psi\sim m_p(f_p/v)\sim2.5$ TeV. This is so because, as is well known from hadron physics, the Skyrmion model overestimates the proton mass by about 30% and this could significantly reduce the signals. The technibaryon mass used in technicolor models has been obtained from the QCD-like one by the inclusion of a factor $\sqrt{N_{\rm TC}/3}$ which is the expected dependence on $N_{\rm TC}$ at leading order in the large-$N_{\rm TC}$ expansion when v is kept fixed. Note also that technibaryons have been taken to be bosons for $N_{\rm TC}$ even and fermions for $N_{\rm TC}$ odd according to the discussion given above. The R_S values have been obtained from the Skyrme model (see [12]). In the QCD-like case, we obtain $R_S=1.57$ TeV^{-1} and this magnitude goes as $\sqrt{N_{\rm TC}}$ in the large-$N_{\rm TC}$ limit when v is kept fixed.

After a quick look at Table I we realize the following simple facts. First, the SSC seems to be much more capable for producing technibaryons than the LHC. As is well known, the competition between these two machines relies on the interplay energy versus luminosity. The SSC, being more energetic, is better for producing heavy objects which may be inaccessible to the LHC, but, because of the better statistics, the LHC is more useful for producing light objects. Concerning our work here, technibaryons are heavy objects with masses of several TeV and therefore the SSC is a more appropriate machine for discovering them, provided they exist. Second, in spite of the different numerical factors appearing in Eqs. (14) and (22), the number of events is not very different in the bosonic and the fermionic case for the SSC. These factors are related with the different number of final states and the different representations of the rotation and isospin groups carried by the scalar and the fermionic technibaryons. However, in the bosonic case the cross section in Eq. (14) is proportional to the β of the technibaryon instead of β^3 as it is in the fermionic case. These two effects compensate each other for a β value of the order of 0.1 which is a typical value of this magnitude at the SSC for low $N_{\rm TC}$. Third, we observe that the reaction $W^+W^-\to T\bar{T}$ is roughly a factor of 2 more efficient than the reaction $ZZ\to T\bar{T}$. This comes because of the different density of these two initial states in the pp collisions. Another general fact is that the number of expected events at the SSC increases with the number of technicolors in spite of the fact that the mass of the technibaryons goes as $\sqrt{N_{\rm TC}}$ in the large-$N_{\rm TC}$ limit with v fixed. This is so because of the R_S^8 factor appearing in the cross sections in Eqs. (14) and (22) which in this limit goes as a $N_{\rm TC}^4$. This is not the case of the LHC since, as the center-of-mass energy is much lower, the number of events over the threshold is very sensitive to its exact position which increases with $N_{\rm TC}$. In other words, we have two contrary effects. The cross section of the subprocess near threshold increases with $N_{\rm TC}$ but the luminosity of a given pp machine at this point decreases very fast with $N_{\rm TC}$ for the initial state considered here. For the SSC the first effect still dominates but the contrary happens at the LHC. Note that the fact that the cross sections of Eqs. (14) and (22) increase with $N_{\rm TC}$ is not in contradiction with the well-known fact that the cross section for baryon-antibaryon annihilation into mesons decreases exponentially with the number of colors. The reason is that this last behavior is appropriate when the baryon velocity is kept fixed in the large-N limit. This is not the case of Eqs. (16) and (22) because there we are considering the cross section at threshold and then the technibaryon velocity β decreases with $N_{\rm TC}$ in the large-$N_{\rm TC}$ limit (see [23] for a detailed discussion about these points).

Finally, the number of the expected events found in this preliminary computation is very encouraging, especially for the SSC case, ranging more or less from $0.5\times10^2-10^3$. However these numbers overestimate the signal that one can expect. The reason is the following: let us consider for example the cross section in Eq. (14) which is proportional to s (the squared center-of-mass energy of the subprocess). According to ChPT this dependence on s is appropriate for values of s not very large in comparison to $16\pi v^2$ and hence it is not appropriate near threshold where most of the events take place at the LHC and SSC (note that the invariant mass at threshold is typically of the order of 5 TeV). In particular, a linear dependence on s violates unitariy at some energy and it overestimated the cross section not only for very large energy events but also at threshold. Note that even near threshold, where the momentum of the (anti)technibaryon is not very large, the momenta of the initial state W_L's is large because of the large mass of the technibaryons. In other words, by the use of very general symmetry arguments we have been able to compute the am-

plitude for producing technibaryons but we do not have the right to extrapolate our results to the high-energy domain where the threshold of the reaction is, and where particular details of the unknown dynamics may play an important role. In fact, this is a general problem which also appears in pion dynamics or in elastic $W_L W_L$ scattering (see [6,17,24] for an extensive discussion of these cases).

In practice, the only way to handle this problem is by the use of some unitarization procedure. Of course, this is not a complete solution of the problem since the unitarization method is not unique, but at least it typically produces more realistic answers than the naive nonunitarized predictions. On the other hand, by comparison of different unitarization methods, one can get a feeling of the relative importance of the unitarity effects in a given physical problem. For these reasons, and with the aim of obtaining a much more realistic prediction than the one in Table I, we will develop in the next section a unitarization program appropriate to the problem of computing the expected number of technibaryons to be produced at the LHC and SSC.

V. UNITARIZATION OF THE AMPLITUDES

In order to unitarize the amplitudes obtained in Sec. III we will start from the Heitler's integral equation [25]. This equation can be derived by the use of the so-called K-matrix method [26] and the interested reader can find a brief exposition of this derivation in Appendix A. The K-matrix method was already used to unitarize the amplitudes in the elastic $W_L W_L$ scattering [6,24] and it was compared with other methods such as the Padé approximant one. This last method cannot be applied directly in our case since the reaction we are considering here is not elastic but we will turn to it later. Following the discussion of Appendix A we can write the Heitler's integral equation

$$\tilde{\mathcal{M}}_{if}=\mathcal{M}_{if}+\frac{i}{2}\sum_{n,k} dR_n(P)\tilde{\mathcal{M}}_{in}\mathcal{M}_{nf}$$
$$=\mathcal{M}_{if}+\frac{i}{2}\sum_{n,k}\langle\tilde{\mathcal{M}}_{in}\mathcal{M}_{nf}\rangle\ . \tag{26}$$

Here $\tilde{\mathcal{M}}_{if}$ and $\mathcal{M}_{if}$ are the unitarized and nonunitarized amplitudes from the initial state $|i\rangle=w^a w^a$ to the final state $|f\rangle=T\bar{T}$. P is the total four-momentum of the reaction and the sum is done over all the possible intermediate physical states of n particles with four-momentum $P_i=(E_i,\mathbf{p}_i)$ being k an index over the other quantum numbers needed to completely define the state. The integral measure is the Lorentz-invariant phase-space one given by

$$dR_n(P)=(2\pi)^4\delta\left[P-\sum_{j=1}^{n}P_j\right]\prod_{i=1}^{n}\frac{d\mathbf{P}_i}{(2\pi)^3 2E_i}\ . \tag{27}$$

Therefore, to obtain the unitarized amplitude we have to do the following steps. First we have to introduce as an input the nonunitarized amplitude which in our case will be the one obtained in Sec. III. Next we have to identify the intermediate states contributing to the second term of the right-hand side (RHS) of Eq. (26) (see Fig. 3 for a symbolic representation of this equation). These states include two longitudinal gauge-boson states, four longitudinal gauge-bosons states etc., and also $T\bar{T}$ states, $2(T\bar{T})$ states, etc. Of course, at some given energy, only the $n(T\bar{T})$ states with the threshold below that energy have to be considered but in the case of the $n2w^a$ states we have in principle to include all of them since in our approximation the w^a are Goldstone bosons and therefore they are massless. In fact we will not go so far and we will only consider $2w^a$ intermediate states. This is so not only for simplicity but also because they are the most important at the energies which are relevant for us. In other words, the main unitarity effect at threshold is the initial-state elastic interactions of the W_L's and other effects such as inelastic initial-state interactions or rescattering will be neglected. As most of the $W_L W_L \to T\bar{T}$ subreactions occur near the threshold at the SSC we think this approximation is good enough for our purposes of giving a realistic estimation of the total number of expected events. Once the appropriate set of intermediate states has been chosen, the next step is the resolution of Heitler's integral equation (in fact it is a coupled system of integral equations) and this in general involves the computation of complicate phase-space integrals.

Let us concentrate now in the scalar case, which is the simplest one, to illustrate in some detail the discussion above. We start from the nonunitarized amplitude that

TABLE I. Number of expected pairs of technibaryons per year at the LHC and SSC. We consider different scenarios (S stands for the scalar cases and F stands for the fermionic cases) and we put in parentheses the number of technicolors. We display also the corresponding values of the radius and the mass of the technibaryon.

Scenario	LHC (W^+W^-)	LHC (Z^0Z^0)	LHC Total	SSC (W^+W^-)	SSC (Z^0Z^0)	SSC Total	R_S (TeV^{-1})	Mass (GeV)
S(2)	5	2	7	28	11	39	1.29	2041
S(4)	5	3	8	172	70	242	1.82	2887
S(6)	3	2	5	411	174	585	2.23	3536
S(8)	1	1	2	684	298	982	2.57	4082
F(3)	3	2	5	59	24	83	1.57	2500
F(5)	1	1	2	181	77	258	2.03	3227
F(7)				327	143	470	2.41	3819
F(9)				460	207	667	2.73	4330

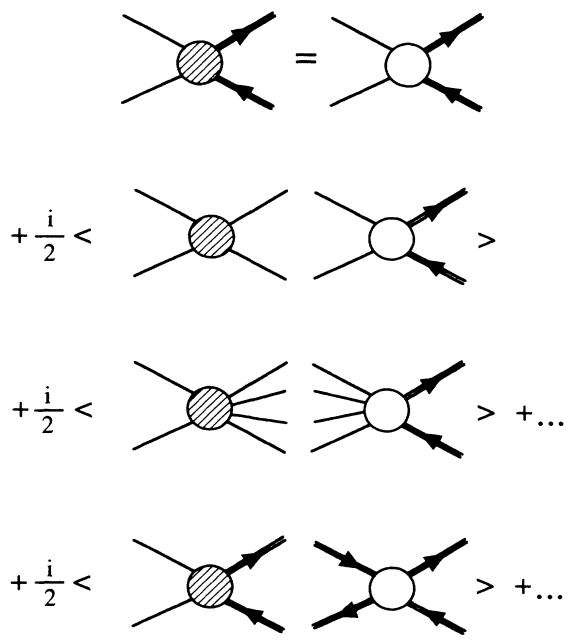

FIG. 3. Pictorial view of Heitler's equation as applied to the unitarization of the $WW \to T\bar{T}$ amplitude.

from Eq. (13) can be written as

$$\mathcal{M}(w^a w^b \to \phi\phi^*) = \frac{2\alpha s}{v^2}\delta_{ab} \ . \tag{28}$$

By using the standard basis for the w^a fields and using the approximation explained below, Eq. (26) reads, in an obvious notation,

$$\begin{aligned}\tilde{\mathcal{M}}(+-,\phi\phi^*) &= \mathcal{M}(+-,\phi\phi^*) \\ &\quad + \frac{i\alpha s}{v^2}\langle \tilde{\mathcal{M}}(+-,+-) + \tfrac{1}{2}\tilde{\mathcal{M}}(+-,00)\rangle \ , \\ \tilde{\mathcal{M}}(00,\phi\phi^*) &= \mathcal{M}(00,\phi\phi^*) \\ &\quad + \frac{i\alpha s}{v^2}\langle \tilde{\mathcal{M}}(00,+-) + \tfrac{1}{2}\tilde{\mathcal{M}}(00,00)\rangle \ .\end{aligned} \tag{29}$$

This equation is interesting because if we know the unitarized amplitudes for $W_L W_L$ scattering, it gives us the unitarized amplitude for $W_L W_L$ going to $T\bar{T}$. Of course, the elastic $W_L W_L$ scattering amplitudes can be obtained as the solution of another equation as the one represented in Fig. 3 but changing the external $T\bar{T}$ legs by $W_L W_L$ legs. This last equation can be solved (considering only $W_L W_L$ intermediate states) by the use of a partial-wave analysis to decouple the different channels and further reconstruction of the amplitudes by addition of the unitarized partial waves until some J value (see for instance [6,24]). Taken into account only the first term in Eq. (2) and the $J=0$ and the $J=1$ waves the following solution is found:

$$\begin{aligned}\tilde{\mathcal{M}}(\alpha\beta,\gamma\delta) &= 16\pi\left[\frac{s/8\pi v^2}{1-is/16\pi v^2}P^0_{\alpha\beta,\gamma\delta}\frac{s/16\pi v^2}{1-is/32\pi v^2}P^1_{\alpha\beta,\gamma\delta}\right. \\ &\quad \left. + \frac{s/48\pi v^2}{1-is/96\pi v^2}3P^2_{\alpha\beta,\gamma\delta}\right] ,\end{aligned} \tag{30}$$

where the nonzero projection constants are $P^0_{+-00} = P^0_{0000} = -P^2_{+-00} = \frac{1}{3}, P^2_{0000} = \frac{2}{3}$. Now we can use this result in Eq. (29) and after some work we obtain the result

$$\tilde{\mathcal{M}}(\alpha\beta \to \phi\phi^*) = \mathcal{M}(\alpha\beta \to \phi\phi^*)\frac{1}{1-is/16\pi v^2} \tag{31}$$

where $\alpha\beta$ stands for the initial standard states $+-$ or 00. Therefore, the unitarized cross section $\bar{\sigma}$ can be written in terms of the nonunitarized ones obtained from Eq. (14) as

$$\begin{aligned}\bar{\sigma}(+- \to \phi\phi^*) &= \bar{\sigma}(00 \to \phi\phi^*) \\ &= \frac{\sigma(+- \to \phi\phi^*)}{1+(s/16\pi v^2)^2} \\ &= \frac{\sigma(00 \to \phi\phi^*)}{1+(s/16\pi v^2)^2} \ .\end{aligned} \tag{32}$$

In the fermionic case, the unitarization of the amplitudes is analogous to the scalar case but, because of the involved Dirac algebra, the computations are more complicated and will be presented in Appendix B. The final result

$$\frac{d\bar{\sigma}}{d(\cos\theta)}(+- \to \psi\bar{\psi}) = \frac{d\bar{\sigma}}{d(\cos\theta)}(00 \to \psi\bar{\psi}) \tag{33}$$

$$= \frac{d\sigma}{d(\cos\theta)}\left[1+\left[\frac{s}{16\pi v^2}\right]^2\frac{1+3\cos^2\theta}{9\cos^2\theta}\right]\Big/\left[1+\left[\frac{s}{16\pi v^2}\right]^2\right] , \tag{34}$$

where the nonunitarized differential cross section is the one in Eq. (22). For the sake of comparison, we plot the unitarized and nonunitarized numerical values of the cross section corresponding to the one-scalar and one-fermionic case in Figs. 4 and 5. With these unitarized cross sections we can repeat the computations done in the preceding section to obtain a more realistic estimation of the number of expected $T\bar{T}$ pairs at LHC and SSC per year. These new results are shown in Table II and will be commented in the next section.

VI. FINAL RESULTS AND DISCUSSION

After the computation with the unitarized amplitudes is done we observe a substantial reduction in the number of expected events, especially in the scalar case. We con-

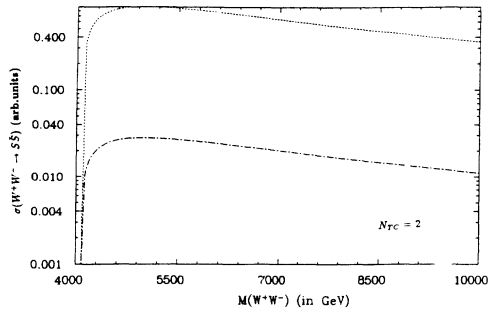

FIG. 4. Cross section for the subprocess $W^+W^- \to \Phi\Phi^*$ vs the invariant mass of the boson pair in arbitrary units. It is displayed in the scenario with $N_{TC}=2$ without unitarization (dotted) and with unitarization (K-matrix method) (dot-dashed).

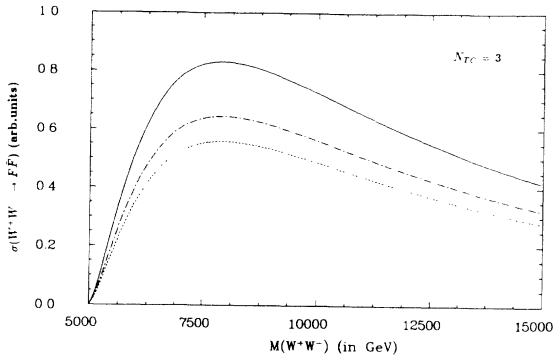

FIG. 5. Cross section for the subprocess $W^+W^- \to \psi\bar{\psi}$ vs the invariant mass of the boson pair in arbitrary units. It is displayed in the scenario with $N_{TC}=3$ without unitarization (solid), with unitarization by the use of the K-matrix method (dotted), and the Padé method (dot-dashed).

sider this fact as a strong evidence in favor of our previous feeling that the unitarization effects could be important and they have to be taken into account in some way. In particular, we arrive at the conclusion that in the scalar case the signal is completely negligible both at the LHC and the SSC. In the fermionic case we obtain a number of events of the order of one hundred per year at the SSC. At the LHC we obtain a very small number of events and hence we consider hopeless this machine for the production of technibaryons. In order to understand why this is the case we show in Figs. 6 and 7 the center-of-mass energy distribution of these expected events. As it was commented above, in spite of the larger luminosity of the LHC, the number of expected events over the $T\bar{T}$ threshold is not as large as in the SSC case since the WW luminosity functions decrease very fast with the fraction of the energy of the initial pp state.

One important issue related with all this discussion is that the unitarization procedure is not unique and therefore there is a lot of arbitrariness in the election of the method one uses to unitarize the amplitudes. For this reason it is a natural question to ask about how strong the dependence of our results is on the unitarization scheme we have used. Trying to answer this question we have also performed our computations with a different method of unitarization as follows. We start from Eq. (29) (or the corresponding to the fermionic case) which make it possible to obtain the unitarized amplitude for the process $W_L W_L \to T\bar{T}$ from the unitarized amplitude of the $W_L W_L$ elastic scattering. Now we can use again this equation but with another different input for the unitarized $W_L W_L$ elastic scattering amplitude. In particular we will consider here the Padé approximant method to unitarize this amplitude previously computed to one loop from the full Lagrangian in Eq. (2) (see [6] for more details). This method has proved to be very appropriate to fit the experimental phase shifts of the $\pi\pi$ elastic scattering and in particular it reproduces very well the effect of the resonances such as the ρ [17]. The Padé method was also applied for the unitarization of the $W_L W_L$ elastic scattering amplitudes [6,24] and probably it is more appropriate than the K-matrix one, at least for QCD-like theories, since it works quite well in the $N_{TC}=3$ case. To apply this method we make the replacement of the partial waves which are polynomials in s (with eventual logarithmic coefficients when one-loop corrections are included) by the higher possible diagonal Padé approximant (the [1,1] in our case) which satisfy the elastic unitarity condition. Then we reconstruct the unitarized amplitude by taking into account the $J=0$ and $J=1$ channels (see [6] for more details). With the unitarized $W_L W_L$ elastic scattering amplitudes obtained in this way we use Eq. (29) (or the corresponding to the fermionic case) to get the new unitarized $W_L W_L \to T\bar{T}$ amplitudes. The number of events obtained in that way for the typical case ($N_{TC}=3$) is 3 at the LHC and 65 at the SSC. The cross sections and the spectra of these events in the W^+W^- channel are shown in Fig. 5 and Fig. 8, respectively.

As is clear from these plots, the Padé method produces

TABLE II. Same description as Table I but now we show the K-matrix unitarized results.

Scenario	LHC (W^+W^-)	LHC (Z^0Z^0)	LHC Total	SSC (W^+W^-)	SSC (Z^0Z^0)	SSC Total	R_S (TeV^{-1})	Mass (GeV)
S(2)				1		1	1.29	2041
S(4)				1	1	2	1.82	2887
S(6)				1	1	2	2.23	3536
S(8)				1	1	2	2.57	4082
F(3)	2	1	3	40	16	56	1.57	2500
F(5)	1	1	2	121	51	172	2.03	3227
F(7)				218	95	313	2.41	3819
F(9)				307	138	445	2.73	4330

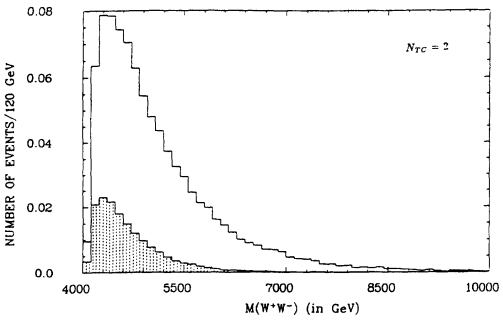

FIG. 6. Center-of-mass energy distribution of the subprocess $WW \to T\bar{T}$ corresponding to the $N_{TC}=2$ scenario for the LHC (dashed) and the SCC (K-matrix unitarized results).

a reduction of the cross section and a number of expected events which is not so large as the K-matrix one (note that in the Padé method we are including the effect of the techni-ρ resonance [6]). This fact suggests that we can consider the K-matrix results more as a lowest bound on the number of expected events than as the real value of this number. Hence, we can consider the results in Table II as conservative predictions in the sense that by using other unitarization methods or none we would obtain a larger number of events.

Once we have some confidence that there will be a large number of $T\bar{T}$ pairs in the fermionic case at the SSC, one has to ask which will be the experimental signature of these events and which will be the possible standard backgrounds to this signature. As was explained in Sec. II the fermionic technibaryons are expected to be massive and (fractional) charged particles. On the other hand one look to the center-of-mass-energy spectra in Figs. 6–8 shows that the typical velocity of the technibaryons produced is not very large so they can be considered in a first approximation as nonrelativistic. The interaction of these heavy particles with ordinary matter will produce many electrons and it will be easy to measure the momentum and the energy of the technibaryons to see its heavy character which will distinguish them from any other conventional particle. Therefore we believe that these events will be essentially free of background. As we will have many of them (see again Table II) they will be in principle easy to catch provided they exist.

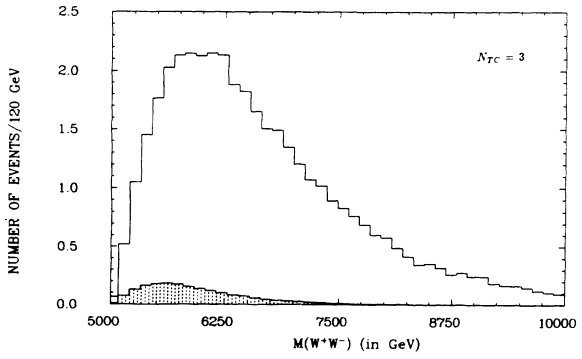

FIG. 7. Center-of-mass energy distribution of the subprocess $WW \to T\bar{T}$ corresponding to the $N_{TC}=3$ scenario for the LHC (dashed) and the SSC (K-matrix unitarized results).

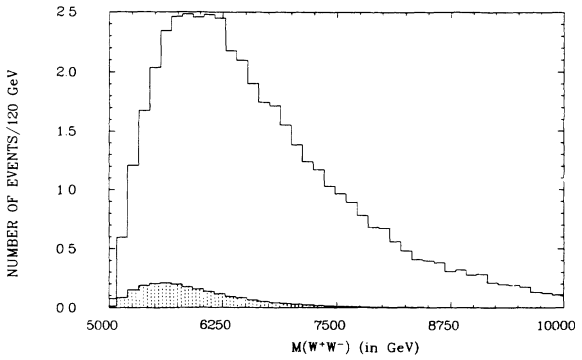

FIG. 8. Center-of-mass energy distribution of the subprocess $WW \to T\bar{T}$ corresponding to the $N_{TC}=3$ scenario for the LHC (dashed) and the SSC (Padé unitarized results).

VII. CONCLUSIONS

The main conclusions of this work can be stated as follows. Technibaryons appear in a very natural way in many strongly interacting symmetry-breaking scenarios of the standard model, being typically very heavy particles. Many properties of these particles can be determined by the use of very general symmetry arguments and we do not have to limit ourselves to any particular model to make important predictions about them.

Of course, in some particular models, other ways for producing technibaryons, different from the one considered here, are possible. In that case the number of expected events will be even larger but, in any case, the mechanism studied in this work will be always present.

In the computation of the number of expected technibaryon pairs at the LHC and SSC the issue of unitarity plays an essential role because the squared energy at threshold is very large (note that the parameter of the chiral expansion is $s/16\pi v^2$) and it requires further study. In any case, even a conservative estimation shows that, if the technibaryons are fermions, many events can be produced at the SSC but not at the LHC. The case of scalar technibaryons is hopeless in both accelerators. Obviously, the negative conclusions apply only for the reaction considered here but not for others that could be present in some particular models.

Finally, because of the clear and background-free signature of these events it will be in principle easy to observe them at the SSC provided technibaryons exist.

Note added. Our attention has been brought to the fact that technibaryons could also be produced through quark-antiquark annihilation via s-channel weak-gauge-boson exchange. Along this work our philosophy has been to describe the low-energy regime of the symmetry-breaking sector of the SM with a nonlinear σ model to exploit the custodial symmetry of this sector. As was explained, we have to make our computations to zero order in the gauge couplings g and g' which is the simplest nontrivial approximation. At this level, the only possible mechanism for producing technibaryons is the one considered by us in this work because the other one men-

tioned above requires having the gauge couplings different from zero. However, it can be argued that this process could be potentially competitive with the production of technibaryons through gauge-boson fusion since the quark luminosity is much larger than the gauge-boson one and this could compensate the extra gauge-coupling factors. In fact it is possible that this was the case if the technibaryons were not so heavy. This is because the quark-antiquark annihilation processes are typically very important at low center-of-mass energies but their amplitudes decrease fast with the energy and probably are not important at the very high energies where the threshold for producing technibaryons pairs is. This is, for instance, the case in gauge-boson pair production (see the fifth reference quoted in [6] and the references quoted there) where gauge-boson fusion dominates over quark-antiquark annihilation at large enough energies. In any case, only a detailed numerical computation has the last word and work is in progress in this direction. It will be very interesting if other mechanisms for producing technibaryons are possible because this could increase the signal but we are not especially optimistic about that.

ACKNOWLEDGMENTS

One of the authors (A.D.) would like to thank S. Dimopoulos and M. J. Herrero for continuous encouragement and T. N. Truong for useful discussions on the unitarity problem. A.D. thanks also the CERN TH-Division for hospitality at the early and final parts of this work. This work has been supported in part by the Ministerio de Educación y Ciencia (Spain) (CICYT Project No. AEN90-0034).

APPENDIX A

For the sake of completeness we include in this appendix the derivation of Heitler's integral equation [25] by the use of the K-matrix formalism [26]. Let S be the scattering matrix and let us parametrize it in terms of a new matrix K in the following way:

$$S=\frac{1-iK/2}{1+iK/2} . \tag{A1}$$

With this parametrization S is unitary if and only if K is Hermitian. In practice the S matrix is typically obtained by the use of some expansion:

$$S=1+S^{(1)}+S^{(2)}+\cdots . \tag{A2}$$

The problem arises because, in spite of the fact that S is unitary, the truncation of the above series at some finite number of terms is not and then probability is not conserved. However, this problem can be avoided in principle by the following technique. We can solve Eq. (A1) to obtain the K matrix as a function of S:

$$K=\frac{i(S-1)}{1+(S-1)/2} . \tag{A3}$$

If we introduce the truncated series of S in this equation, we will obtain another truncated series for the K matrix,

$$K=K^{(1)}+K^{(2)}+\cdots , \tag{A4}$$

and if we use this truncated series in Eq. (A1) we will have a new series for the S matrix which is unitary to any order:

$$S=1+\tilde{S}^{(1)}+\tilde{S}^{(2)}+\cdots . \tag{A5}$$

Now it is not difficult to express the terms of the K series as a function of the terms of the old S series up to the same order:

$$K^{(n)}=i\sum_{p=1}^{n}(-\tfrac{1}{2})^{p-1}\times\sum_{n_1+n_2+\cdots+n_p=n}S^{(n_1)}S^{(n_2)}\cdots S^{(n_p)} . \tag{A6}$$

At lowest order we have $K^{(1)}=iS^{(1)}$ and by using Eq. (A1) and Eq. (A2) we arrive at

$$\tilde{S}^{(1)}=S^{(1)}+\tfrac{1}{2}\tilde{S}^{(1)}S^{(1)} . \tag{A7}$$

Let us consider now some initial state $|i\rangle$ and some final state $|f\rangle$ orthogonal to it and let $S_{if}^{(1)}$ be the corresponding matrix element of $S^{(1)}$ ($S_{if}^{(1)}=\langle i|S^{(1)}|f\rangle$). Then we can express $S_{if}^{(1)}$ (and $\tilde{S}_{if}^{(1)}$ with the same notation) in the usual way as

$$\begin{aligned} S_{if}^{(1)}&=i(2\pi)^4\delta(P_i-P_f)\mathcal{M}_{if} ,\\ \tilde{S}_{if}^{(1)}&=i(2\pi)^4\delta(P_i-P_f)\tilde{\mathcal{M}}_{if} , \end{aligned} \tag{A8}$$

where P_i and P_f are the momenta of the initial and the final state, respectively, and $\tilde{\mathcal{M}}_{if}$ and $\mathcal{M}_{if}$ are the unitarized and the nonunitarized amplitudes of the process. By use of Eqs. (A7) and (A8) we finally obtain Eq. (26).

APPENDIX B

Here we show some details of the derivation of the result in Eq. (34) for the unitarized cross section in the fermionic case ($W_L W_L\to\psi\bar{\psi}$). We start from the nonunitarized amplitude in Eq. (18). From the low-energy expansion of the propagators in Eq. (20) and recalling that in our case $\epsilon_{abc}=0$ we have

$$\mathcal{M}=\frac{4}{s^2}\left[\frac{km_\psi}{v}\right]^2(u-t)Au_1\not{p}_1v_2 , \tag{B1}$$

where we have used the fact that, for $a=b$, $A=B$ and that the spinors u_1 and v_2 satisfy the free Dirac equation. Then Heitler's integral equation at the same level of approximation used in the scalar case reads

$$\begin{aligned} \tilde{\mathcal{M}}(+-,\psi\bar{\psi})&=-\frac{16}{s^2}\left[\frac{km_\psi}{v}\right]^2\left[\frac{s-4m_\psi^2}{s}\right]^{1/2}\bar{u}_1\Gamma_{+-}v_2 ,\\ \tilde{\mathcal{M}}(00,\psi\bar{\psi})&=-\frac{16}{s^2}\left[\frac{km_\psi}{v}\right]^2\left[\frac{s-4m_\psi^2}{s}\right]^{1/2}\bar{u}_1\Gamma_{00}v_2 , \end{aligned} \tag{B2}$$

where

$$\Gamma_{+-} = A_{+-} \not{p}_a \cos\theta + \frac{i}{2}\langle \tilde{\mathcal{M}}(+-,+-) A_{+-} \not{p}_c \cos\theta' + \tfrac{1}{2}\tilde{\mathcal{M}}(+-,000) A_{00} \not{p}_c \cos\theta' \rangle \ , \tag{B3}$$

$$\Gamma_{+00} = A_{+-} \not{p}_a \cos\theta + \frac{i}{2}\langle \tilde{\mathcal{M}}(00,+-) A_{+-} \not{p}_c \cos\theta' + \tfrac{1}{2}\tilde{\mathcal{M}}(00,00) A_{00} \not{p}_c \cos\theta' \rangle \ .$$

In these formulas p_a and p_c are the momenta of one of the incoming and one of the intermediate W_L, respectively, θ' is the angle between the + or $0W_L$'s in the intermediate state and ψ, and the standard basis has been used for the $A=B$ isospin factors. Now we proceed as in the scalar case. First we introduce into the above equations the unitarized amplitudes for elastic $W_L W_L$ scattering in Eq. (30). Then we compute the phase-space integrals over the intermediate-state variables which are more complicated now and finally we use REDUCE to compute the squared modulus of the unitarized amplitudes:

$$|\tilde{\mathcal{M}}(+-\to\psi\bar{\psi})|^2 = |\tilde{\mathcal{M}}(00\to\psi\bar{\psi})|^2 = 16\left[\frac{km_\psi}{v}\right]^4\left[\frac{s-4m_\psi^2}{s}\right]\frac{\cos^2\theta+(1/9)(s/16\pi v^2)^2(1+3\cos^2\theta)}{1+(s/16\pi v^2)^2} \ . \tag{B4}$$

[1] J. M. Cornwall, D. N. Levin, and G. Tiktopoulos, Phys. Rev. C **10**, 1145 (1974); B. W. Lee, C. Quigg, and H. Thacker, *ibid.* **16**, 1519 (1977); M. Veltman, Acta Phys. Pol. B **8**, 475 (1977); T. Appelquist and C. Bernard, Phys. Rev. D **22**, 200 (1980).

[2] M. S. Chanowitz and M. K. Gaillard, Nucl. Phys. **B261**, 379 (1985).

[3] P. Sikivie *et al.* Nucl. Phys. **B173**, 189 (1980).

[4] S. Weinberg, Physica **96A**, 327 (1979).

[5] J. Gasser and H. Leutwyler, Ann. Phys. (N.Y.) **158**, 142 (1984).

[6] A. Dobado and M. J. Herrero, Phys. Lett. B **228**, 495 (1989); **233**, 505 (1989); A. Dobado, M. J. Herrero, and T. N. Truong, *ibid.* **235**, 129 (1989); A. Dobado, M. J. Herrero, and J. Terron, Z. Phys. C **50**, 205 (1991); **50**, 465 (1991); A. Dobado, M. J. Herrero, and J. Terrón, in *Proceedings of the ECFA Large Hadron Collider Workshop,* Aachen, Germany, 1990, edited by G. Jarlskog and D. Rein (CERN Report No. 90-10, Geneva, Switzerland, 1990), Vol. II, p. 360.

[7] T. H. R. Skyrme, Proc. R. Soc. London **260**, 127 (1961); Nucl. Phys. **31**, 556 (1962).

[8] G. S. Adkins, C. R. Nappi, and E. Witten, Nucl. Phys. **B228**, 552 (1983).

[9] J. M. Gipson and H. C. Tze, Nucl. Phys. **B183**, 524 (1981); J. M. Gipson, *ibid.* **B231**, 365 (1984).

[10] E. Witten, Nucl. Phys. **B223**, 422 (1983); **B223**, 433 (1983).

[11] E. D'Hoker and E. Farhi, Phys. Lett. **134B**, 86 (1984); Nucl. Phys. **B241**, 109 (1984).

[12] A. Dobado and J. Terrón, Phys. Lett. B **247**, 581 (1990).

[13] M. F. Atiyah and N. S. Manton, Phys. Lett. B **222**, 438 (1989).

[14] S. Dawson and S. Willenbrock, Phys. Rev. Lett. **62**, 1232 (1989); M. Veltman and F. J. Yndurain, Nucl. Phys. **B325**, 1 (1989).

[15] E. Farhi and L. Susskind, Phys. Rep. **74**, 277 (1981); S. Dimopoulos and L. Susskind, Nucl. Phys. **B155**, 237 (1979).

[16] J. F. Donoghue, C. Ramirez, and G. Valencia, Phys. Rev. D **38**, 2195 (1988).

[17] A. Dobado, M. J. Herrero, and J. N. Truong, Phys. Lett. B **235**, 134 (1990).

[18] J. Ambjorn and V. A. Rubakov, Nucl. Phys. **B256**, 434 (1985); G. Eilam, D. Klabucar, and A. Stern, Phys. Rev. Lett. **56**, 1331 (1986); G. Eilam and A. Stern, Nucl. Phys. **B294**, 775 (1987); Y. Brihaye and J. Kunz, Z. Phys. C **41**, 663 (1989).

[19] G. 't Hooft, Phys. Rev. Lett. **37**, 8 (1976).

[20] M. G. Clements and S. H. Henry Tye, Phys. Rev. D **33**, 1424 (1986).

[21] E. Eichten *et al.*, Rev. Mod. Phys. **56**, 579 (1984).

[22] S. Dawson, Nucl. Phys. **B249**, 42 (1985).

[23] E. Witten, Nucl. Phys. **B160**, 57 (1979).

[24] D. A. Dicus and W. Repko, Phys. Lett. B **228**, 503 (1989); Phys. Rev. D **42**, 3660 (1990).

[25] W. Heitler, Proc. Cambridge Philos. Soc. **37**, 291 (1941).

[26] S. N. Gupta, *Quantum Electrodynamics* (Gordon and Breach, New York, 1981).

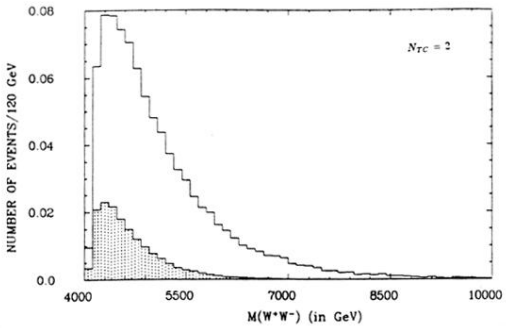

FIG. 6. Center-of-mass energy distribution of the subprocess $WW \to T\bar{T}$ corresponding to the $N_{\mathrm{TC}}=2$ scenario for the LHC (dashed) and the SCC (K-matrix unitarized results).

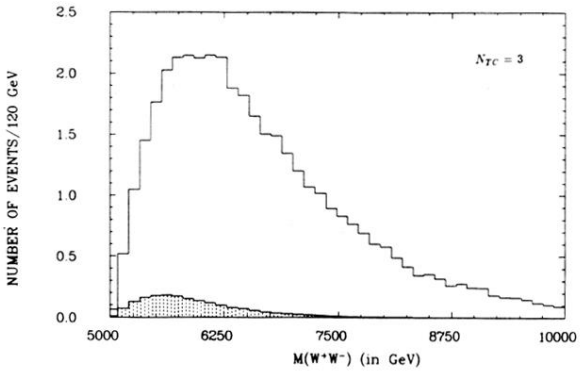

FIG. 7. Center-of-mass energy distribution of the subprocess $WW \to T\bar{T}$ corresponding to the $N_{\mathrm{TC}} = 3$ scenario for the LHC (dashed) and the SSC (K-matrix unitarized results).

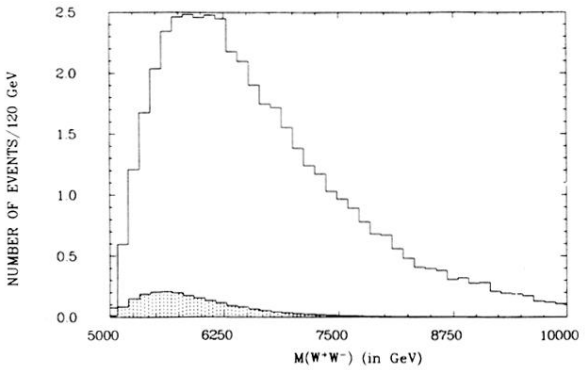

FIG. 8. Center-of-mass energy distribution of the subprocess $WW \to T\bar{T}$ corresponding to the $N_{TC}=3$ scenario for the LHC (dashed) and the SSC (Padé unitarized results).